A modified image enhancement algorithm based on color constancy

Cheng Li (李 成)*, Shan Gao (高 山), and Duyan Bi (毕笃彦)

Signal and Information Processing Lab, Engineering College of Air Force Engineering University, Xi'an 710038, China

**E-mail: ecm_li@163.com*

Received April 27, 2009

According to the color constancy theory, a modified variation Retinex is proposed for improving the visibility of the dark regions in images under insufficient and/or non-uniform lighting conditions. A new penalty functional based on nonlinear diffusion and correlation between the reflectance and the given image is designed for the intensity image enhancement, followed by adaptive color compensation. With high computational efficiency achieved by an improved multi-resolution algorithm, simulation results prove that the proposed method shows more colorful and vivid visual performance, and achieves wider dynamic range with higher objective standard values.

OCIS codes: 100.0100, 100.2980, 330.1720.

doi: 10.3788/COL20090709.0784.

Color is actually not an attribute that can be attached to the objects but basically a result of the processing done by the brain and the retina. The human visual system has such an ability that can determine the colors of objects irrespective of the illuminant, which is called color constancy[1]. As the computational model, the Retinex theory considers that color perception by human eyes does not depend on the light reflected by the object, but correlates with integrated reflectance. The formation of a given image S can be decomposed into two parts: the reflectance image R and the illumination image L, and at each pixel $S(x, y) = R(x, y) \times L(x, y)$. The goal of the Retinex is to bring out the reflectance part which reveals the truth of the scene or object, and lead to improve the brightness, contrast, and high dynamic range of image. For images suffering from insufficient and/or non-uniform lighting leading to dark regions containing information, Retinex is the very solution. Since its foundation, Retinex algorithms have gone through three typical periods. Following the two random walk types by Land[2] and a series of center/surround opponent operations by Jobson *et al.*[3], Kimmel *et al.*[4] proposed a variational framework that unifies many previous ones, and concluded the estimation of L to a Quadratic Programming (QP) optimization problem by minimizing the energy functional via its related Euler-Lagrange (E-L) equations.

Retinex algorithms firstly convert the three components to the logarithmic domain with the multiplication changing into addition, which are $s = l + r$, s=log(S), l=log(L), and r=log(R). Kimmel *et al.* brought about the variational framework via[3]

$$\min\ \{F[l]\} = \int_{\Omega} (|\nabla l|^2 + \alpha|l - s|^2 + \beta|\nabla(l - s)|^2)\mathrm{d}x\mathrm{d}y,$$
$$\text{s.t. } l \geq s \text{ and } \langle \nabla l, \vec{n} \rangle = 0 \text{ on } \partial\Omega, \quad (1)$$

where Ω is the support of the image, $\partial\Omega$ is its boundary, $\vec{n}$ is the normal to the boundary, α and β are free nonnegative real parameters. Three penalty terms in $F[l]$ force l's smoothness, proximity between l and s, and r's smoothness, respectively. The numerical process of Eq. (1) employs the Projected Normalized Steepest Descent (PNSD) with a NSD iteration format.

Because of the equivalence between the Gaussian kernel and solution to the heat diffusion equation, Partial differential equation (PDE)-based approaches[5] offer a good summary and provide a good tool for the Retinex algorithm. However, for failing to reconstruct piecewise constant illumination with a linear diffusion process, Kimmel's variational Retinex suffers from artificial halos and color distortion. Several methods[6] based on the nonlinear diffusion process combined into the time-evolution presented better performances, but they were not reasonable enough to be related with the basic assumptions which lead to constructions of the energy functional.

To cope with this basic problem, another new modified nonlinear diffusion term is considered especially as well as high iteration efficiency in the letter. We present the algorithm in HSI color-space for its simplicity as the classical intuitive color system, and compare its performance with other previous algorithms' on the basis of subjective and objective standards. The intensity component image I is enhanced by the proposed modified variational Retinex, and the S component image is adaptively adjusted with the H one remaining the same.

Global spatial smoothness of the luminance image is the basic assumption in Retinex theory. Especially, the third item in Eq. (1) assures the reflectance's smoothness, but the Bayesian penalty expression is at a certain loss of detail and edge's information. Because $\int |\nabla X|^2$ as the smoothness' realization focuses much on decreasing the gradient norm, and would impose bad effects on discontinuous jump in the reflectance r. As it is forced upon in Kimmel's algorithm, it would blur the r and cause artificial halos. So another basic assumption should be considered that an item reflect the r's boundary based on gradient norm. And we deem that information in the gradient domain of the reflectance r and the given image s has a high correlation. Hence, we modify the penalty functional in Eq. (1) by replacing the third item with a

new nonlinear diffusion one $|\nabla(l-s)|^2|\nabla s|^2$ to preserve the detail-and-edge information of r. Combined with the correlation between r and s, the modified energy functional is formulated as

$$\min_l \{F[l]\} = \int_\Omega \Big(|\nabla l|^2 + \alpha|l-s|^2 - \beta|\nabla(l-s)|^2|\nabla s|^2\Big)\mathrm{d}x\mathrm{d}y,$$
$$\text{s.t. } l \geq s \text{ and } \langle \nabla l, \vec{n}\rangle = 0 \text{ on } \partial\Omega, \quad (2)$$

where β is the parameter to adjust the correlation stated above. Obviously, minimization of the $F[l]$ calls for subtraction of such a correlation from it, that is why there exists a subtraction sign before the third item in Eq. (2).

The energy functional is solved via the E-L equation, which is given by

$$EL(l) = \alpha(l-s) - \Delta l + \beta \mathrm{div}(|\nabla s|^2 |\nabla(l-s)|) = 0 \text{ (s.t. } l \geq s). \quad (3)$$

In Eq. (3), the third item provides nonlinear diffusion process, for $|\nabla s|^2$, the conductive coefficient or edge-stopping function, is dependent on the image. In Ref. [6], P_M diffusion is introduced by the second-order edge-stopping function, which tends to cause blocky effects and false edges. Compared with it, we put more attention on the correlation of gradient information between s and r, deem that the edges and details of the r derive from s, and replace the so-called anisotropic function by the norm of s, which can not only preserve the edge information, but also eliminate the blocky effects caused by edge effects. With the result, the performance is in proximity to the fourth-order PDEs but with less complexity apparently.

To solve the Eq. (3), we also introduce the artificial time-variable t transforming it into the gradient descent flow or so-called time-evolution equation described as

$$\partial l/\partial t = -[\alpha(l-s) - \Delta l + \beta \mathrm{div}(|\nabla s|^2 |\nabla(l-s)|)] \text{ (s.t. } l \geq s). \quad (4)$$

Projecting onto the constraint $l \geq s$ is done by max (l_n, s) in the iteration. The proposed nonlinear diffusion considers both of edge-preservation and diffusion effects, assuring the piecewise constant illumination and reflectance.

Equation (4) converges slowly, and we also have to apply the multi-resolution solution which was firstly used by McCann[7]. From estimating the coarsest resolution to the finest one, few iterations at each level are enough for convergence[4]. The pyramid of image s should be firstly constructed, Kimmel used the Gaussian kernel convolution to smooth the image, but it is the linear diffusion process with a lot of drawbacks, most importantly, the great loss of edge information. The construction of scale-space should keep the edge-detail which dose a good job for estimation loop at each resolution layer. So, we apply the regularized P_M for pyramid construction which further transforms the assumption that l be smooth to that l be piecewise smooth ab ovo, and this will do work in further. The sampling is by 2:1 ratio, that is to say, the average value of the four-neighboring block substitutes it.

For better contrast, linear diffusion takes place of the Gaussian kernel which acts as only once in the iteration. The two iteration times are both set to 10. For regularized P_M, we choose the second edge-stopping function $c = 1/[1 + (|\mathrm{grad}\ (I)\ |/K)^2]$, and other parameters are $K = 10$, $\mathrm{d}t = 0.2$, and $\sigma^2 = 0.1$. The results are shown in Fig. 1, from which we can see more details in every layer of the latter one.

After the initialization, the numerical process of Eq. (4) is conducted, there is no other special about the numerical scheme which is of little key points except 1) the initial condition is set to the maximum of the image; 2) when updating the next resolution layer, the result is up scaled (2:1 ratio) by pixel replication in the neighborhood. By the multi-resolution solution based on regularized P_M, we can obtain more edged and vivid images than precious pyramid-construction.

In HSI color space, it is easy and indispensable to retouch the S component for color compensation. The aim can be achieved by histogram equalization, median filtering, gamma correction etc. On the basis of above methods, we bring about an adaptive method as

$$S_a(x,y) = \begin{cases} k \cdot S(x,y) & \text{if } k > Thr, \\ S(x,y) & \text{else} \end{cases}$$
$$k = I_a(x,y) \cdot I_{a\_AV}/I^2(x,y), \quad (5)$$

where I_{a_AV} is the mean of the enhanced I component I_a; k acts as the adaptive coefficient, which may be rewrote as $k = [I_a(x,y)/I(x,y)] \cdot [I_{a\_AV}/I(x,y)]$ containing two parts: the former is the enhanced ratio of I component defined as k_I, and the latter is the adjustment for k_I. The construction of k reflects the composition of global and local impact. And the Thr is also set to 1[8]. With the adaptive k will validate the basic idea in Ref. [8] that is the enhancement of S component in proportion to the enhanced ratio of I component would make the color clearer.

For the image quality assessment evaluating Retinex algorithms' performance, subjective quality metrics behave best, and there also have been many objective measures such as Mean, Variance, Entropy, Structural Similarity (SSIM) and so on[9,10]. Definition is also an efficient standard conducted in the gradient domain, especially for evaluating the degree of details and contrasts of the image. In the letter, we apply it to quantify the degree of visibility improvement achieved by different Retinex algorithms and it is given by

$$\mathrm{Def} = \frac{1}{MN}\sum_{m=1}^{M}\sum_{n=1}^{N}\sqrt{(I_x(m,n))^2 + (I_y(m,n))^2}, \quad (6)$$

where I_x, I_y are two direction gradients of a given image $I(m,\ n)$ with the size of $[M,\ N]$. Gradient can be calculated by central difference to obtain two-order precision. Actually, the bigger the definition value is, the clearer the image is achieved.

We apply the proposed algorithm to several typical testing images which suffer from bad illumination, low dynamic range, and off-color tone. Parameters for the Pyramid construction are the same as these stated in Fig. 1. Typical results correspond to $\alpha = 0.0001$ and $\beta = 0.1$, which is similar to Kimmel's, but there is

different performance on enhancement. And we also involve the alternative illumination correction by Gamma correction used in Kimmel's Retinex. The only parameter γ is set during the process. The number of resolution layer changes with the size of image by the largest power of 2. When meeting the odd num of row or column, we expand the image to the nearest dimension of even size. And the size of 5×5 is set to be the smallest block for the coarsest resolution.

Firstly, we compare the difference between two variational frameworks, with the same parameters for testing synthetic images. We can see the different performance of them in Fig. 2. There are more sharp edges we can obtain than the Kimmel's, just for the nonlinear diffusion introduced in the $F[l]$. Then, we compare the proposed algorithm with both MSRCR and Kimmel's Retinex for natural images. We apply the TruView's Photo Flair to evaluate the MSRCR, with the "Scenic Mode, Default scales (5 20 240), autolevel and white balance", we could see that it has already partially restrained MSRCR's drawbacks such as colors shifting to gray because of gray-world assumption. Parameters for Kimmel's are set to default as in Ref. [4] during the multi-resolution algorithm and post-processing. While our proposed algorithm in HSI color-space with much bigger value of γ, which could bring less effect of illumination image L. From the results in Figs. 3 and 4, we can see that our algorithm could present more vivid high-contrast enhanced image, especially in the dark regions, achieving the dynamic range compression. And for choosing the HSI color space and adaptive adjustment of S component, we obtain more colorful results avoiding color distortion.

Fig. 1. Two pyramid constructions with 10-time iteration.

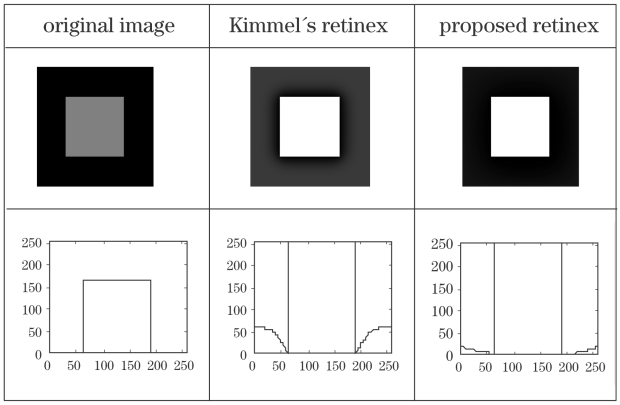

Fig. 2. Synthetic images to test performance.

Except for subjective evaluation, the typical objective evaluation values are in list in Table 1. With common standards for global and local contrast, the proposed algorithm offers better results than others'. And further experiments witness that the proposed algorithm is stable for a wide range of α, β in Fig. 5 and Table 2.

In conclusion, a modified variation Retinex based on nonlinear diffusion in the HSI color space is introduced. We focus more on the correlation between the reflectance image and the given image, and modify the multi-resolution algorithm by adopting the regularized P_M for pyramid construction. With the adaptive adjustment of S component, experimental results give better visible enhanced images with wider dynamic range and vivid color. And further application such as haze removal and shadow removal etc. will be conducted with the proposed algorithm to validate its efficiency.

Table 1. Objective Evaluations

Fig. 3 "Girl"	Original image	MSRCR	Kimmel's	Proposed
Mean	61.7563	79.0505	118.2644	126.8826
Variance	67.5909	68.14	55.375	66.5674
Definition	9.9881	18.9286	13.4213	19.5995
Fig. 4 "Ben"	Original image	MSRCR	Kimmel's	Proposed
Mean	74.9878	85.7159	136.3939	125.3696
Variance	56.8752	59.5649	51.7086	62.7979
Definition	9.8999	14.0311	12.0999	14.3809

Table 2. Objective Evaluations for Robust Evaluation

Fig. 5 "Girl"	α=1, β=0.1, γ=2.2	α=0.0001, β=0.0001, γ=2.2
Mean	111.7442	97.9513
Variance	62.7043	67.1937
Definition	13.649	15.2743

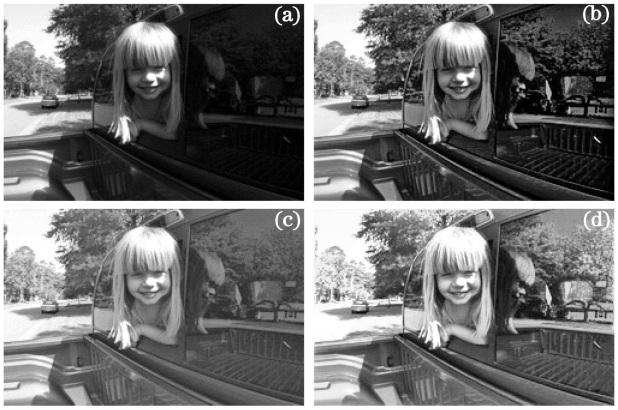

Fig. 3. Enhanced results for "Girl". (a) Input image, (b) PhotoFlair's MSRCR, (c) Kimmel's Retinex, and (d) proposed algorithm (γ=5).

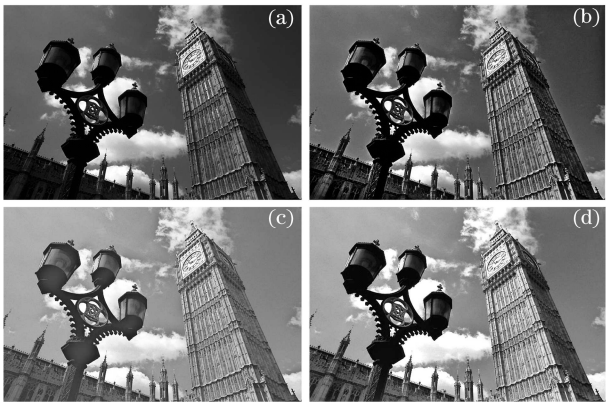

Fig. 4. Enhanced results for "Ben". (a) Input image, (b) PhotoFlair's MSRCR, (c) Kimmel's Retinex, and (d) proposed algorithm (γ=3).

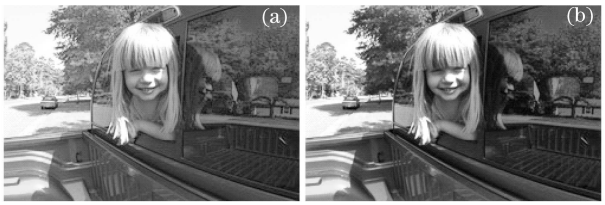

Fig. 5. Robust evaluation. (a) α=1, β=0.1, γ=22, (b) α=0.0001, β=0.0001, γ=2.2.

This work was supported by the National "863" Project of China under Grant No. 2007AA701121 and the NDS&T's Key Laboratory Foundation under Grant No. X80c6106.

References

1. M. Ebner, *Color Constancy* (John Wiley & Sons Ltd., Chichester, 2007).
2. E. H. Land and J. J. McCannm, J. Opt. Soc. Am. **61,** 1 (1971).
3. D. J. Jobson, Z. Rahman, and G. A. Woodell, IEEE Trans. Image Processing **6,** 451 (1997).
4. R. Kimmel, M. Elad, D. Shaked, R. Keshet, and I. Sobel, International Journal of Vision **52,** 7 (2003).
5. G. Chen, K. Yang, R. Chen, and Z. Xie, Chin. Opt. Lett. **6,** 648 (2008).
6. H. Takahashi, T. Saito, and T. Komatsu, in *Proceedings of 2006 ICIP* 977 (2006).
7. B. Funt, F. Ciurea, and J. J. McCann, Journal of Electronic Imaging **13,** 48 (2004).
8. D. H. Choi, I. H. Jang, and M. H. Kim, in *Proceedings of ISCAS* 3948 (2007).
9. K. R. Joshi and R. S. Kamathe, in *Proceedings of ICALIP* 1229 (2008).
10. J. Pang, R. Zhang, H. Zhang, X. Huang, and Z. Liu, Chin. Opt. Lett. **6,** 491 (2008).